Electronic Supplementary Material (ESI) for Journal of Materials Chemistry C.

Supplementary information
The Impact of Stacking and Phonon Environment on Energy Transfer in Organic Chromophores: Computational Insights

Aliya Mukazhanova,[1] Hassiel Negrin Yuvero[2], Victor M. Freixas,[2] Sergei Tretiak,[3] Sebastian Fernandez-Alberti[2], Sahar Sharifzadeh[1,4]

[1] Division of Materials Science and Engineering, Boston University, USA
[2]Universidad Nacional de Quilmes/CONICET, Argentina
[3] Theoretical Division and Center for Integrated Nanotechnologies, Los Alamos National Laboratory, USA
[4] Department of Electrical and Computer Engineering, Boston University, USA

1. Transition densities of molecules from the AM1 Hamiltonian

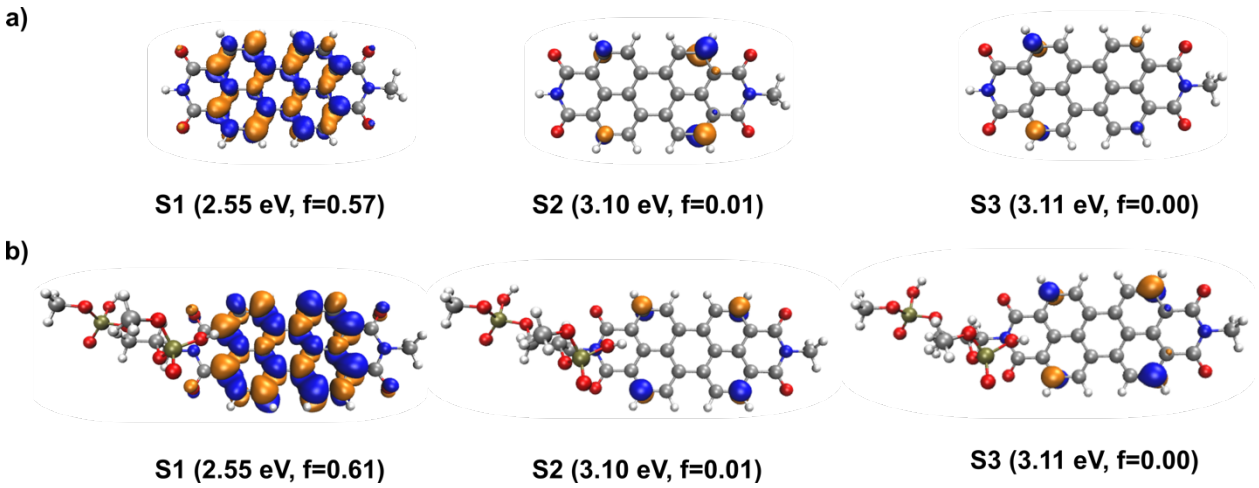

Figure S1. Transition density of optimized geometries of a) monomer b) monomer with backbone

The electronic transition density localization of lowest four excited states of monomer molecules are shown on Figure S3. The backbone does not affect the excited state energetics in case of monomer. The S1 is delocalized across the perylene core while S2 and S3 are localized on specific sites.

Figure S2 presents electronic transition density of three lowest excited states of dimer molecules. For both dimer molecules the first (S1) and the second (S2) states are delocalized across the perylene core while the third (S3) state is localized on specific sites. For both dimer molecules, the S1 has a less significant oscillator strength compared to S2. The fact that S2 state has a significant oscillator strength represents the parallel orientations of PDI monomers, like in typical H-like aggregates. Interestingly, the addition of the backbone increases the oscillator strength of S2 state (Figure S2b). Thus, it is expected that the S2 state of the dimer with backbone will be brighter than the S2 state of pristine dimer.

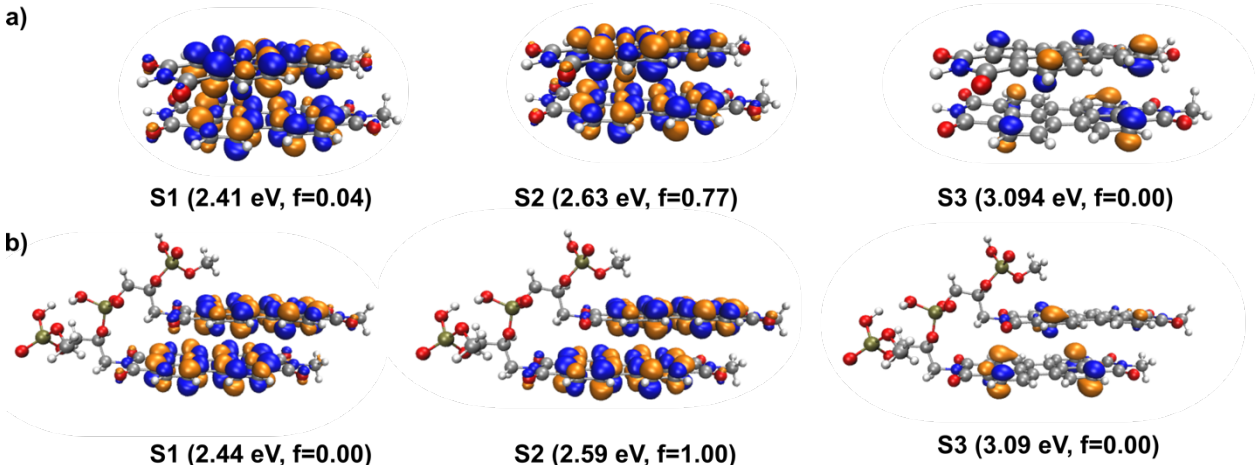

Figure S2. Transition density of optimized geometries of a) dimer b) dimer with backbone

The electronic transition density localization of four excited states of trimer molecules is shown on Figure S3. The S1 and S3 are delocalized across the three perylene cores while S2 is localized on top and bottom perylene cores and S4 is localized on specific sites. Excited state electronic energies E_{S_i} and transition density spatial localizations for each S_i state for the PDI dimer and trimer, shown in Figure 2 and figure 3 can be rationalized using the Frenkel exciton model (see below).

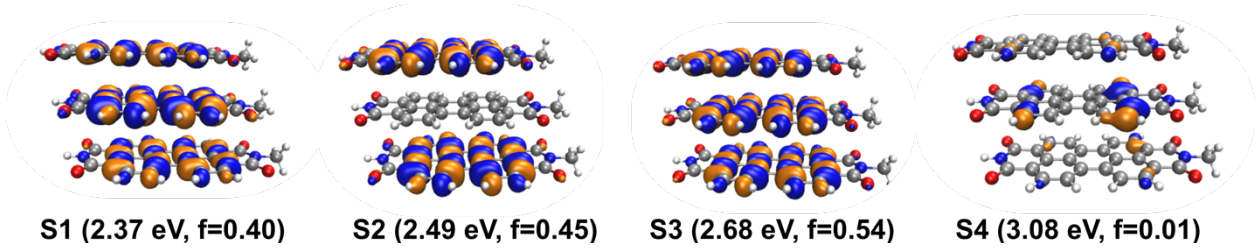

Figure S3. Transition density of optimized geometries of trimer

2. Comparison of absorption spectra calculated with different levels of theory

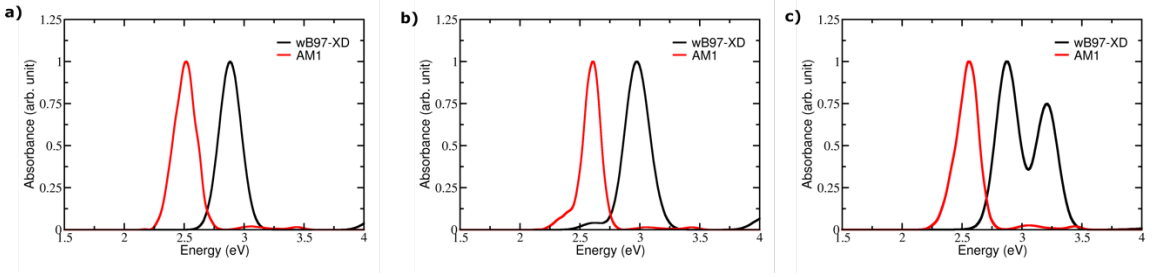

Figure S4. Comparison of absorption spectra calculated with AM1 semi-empirical Hamiltonian and wB97-XD functional

3. Frenkel exciton model for perylene diimide dimer and trimer

In the case of the dimer, we can write S_1 and S_2 solutions as linear combinations of the state S_1 of each monomer. Let us suppose that, for the monomer, S_1 has energy E and V is the corresponding coupling between both two parallel monomers. The Frenkel Hamiltonian matrix H_2 reads as:

$$H_2 = \begin{pmatrix} E & V \\ V & E \end{pmatrix}$$

with the corresponding eigenvalues:

$$E_{S_1} = E - V$$
$$E_{S_2} = E + V$$

and the associated eigenvectors:

$$\begin{pmatrix} -1 & 1 \end{pmatrix}$$
$$\begin{pmatrix} 1 & 1 \end{pmatrix}$$

These eigenvectors are in agreement with figure 2, that shows the transition density of S_1 and S_2 states evaluated at the optimized geometries of the PDI dimer. Furthermore, since the solution for S_1 state results from opposite combinations of each monomer solution, the corresponding transition dipole moment has two opposite contributions from the individual transition dipole moments of each monomer, yielding a low oscillator strength for S_1 in the dimer, as shown in figure 4. For S_2 state we have the opposite scenario and both individual monomer's transition dipole moments are in the same direction, rising the oscillator strength of S_2 in the dimer to approximately twice the one of S_1 in the monomer.

In the case of the PDI trimer, the Frenkel exciton Hamiltonian can be written as :

$$H = \begin{pmatrix} E & V_1 & V_2 \\ V_1 & E & V_1 \\ V_2 & V_1 & E \end{pmatrix}$$

where E is the energy of the S_1 state for each monomer, V_1 is the coupling between adjacent monomers and V_2 is the coupling between the top and bottom monomers. The corresponding eigenvalues are:

$$E_{S_1} = \frac{1}{2}\left(2E + V_2 - \sqrt{8V_1^2 + V_2^2}\right)$$
$$E_{S_2} = E - V_2$$
$$E_{S_3} = \frac{1}{2}\left(2E + V_2 - \sqrt{8V_1^2 + V_2^2}\right)$$

where now E_{S_1}, E_{S_2} and E_{S_3} are the energies corresponding respectively to S_1, S_2 and S_3 of the trimer. The corresponding eigenvectors are:

$$\left(1 \quad -\frac{4V_1^2 - V_2^2 - V_2\sqrt{8V_1^2 + V_2^2}}{V_1\left(\sqrt{8V_1^2 + V_2^2} - 3V_2\right)} \quad 1\right)$$

$$(-1 \quad 0 \quad 1)$$

$$\left(1 \quad \frac{4V_1^2 - V_2^2 + V_2\sqrt{8V_1^2 + V_2^2}}{V_1\left(\sqrt{8V_1^2 + V_2^2} + 3V_2\right)} \quad 1\right)$$

In analogy to the dimer, all individual transition dipole moments are aligned only for S_3 in the trimer and therefore is the one having the bigger oscillator strength, as shown in figure 4. Furthermore there are no contributions from the middle monomer to S_2, as shown in figure 3.

4. Excited state energies

Table S1. Dimer excited state energies

Excited State	Dimer	Dimer with backbone
S1	2.41	2.44
S2	2.63	2.59
S3	3.09	3.09
S4	3.10	3.10
S5	3.11	3.11
S6	3.11	3.11

Table S2. Trimer excited state energies

Excited State	Trimer
S1	2.37
S2	2.49
S3	2.68
S4	3.08
S5	3.10
S6	3.10
S7	3.10

S8	3.11

5. Non-adiabatic coupling terms for monomer, dimer and trimer

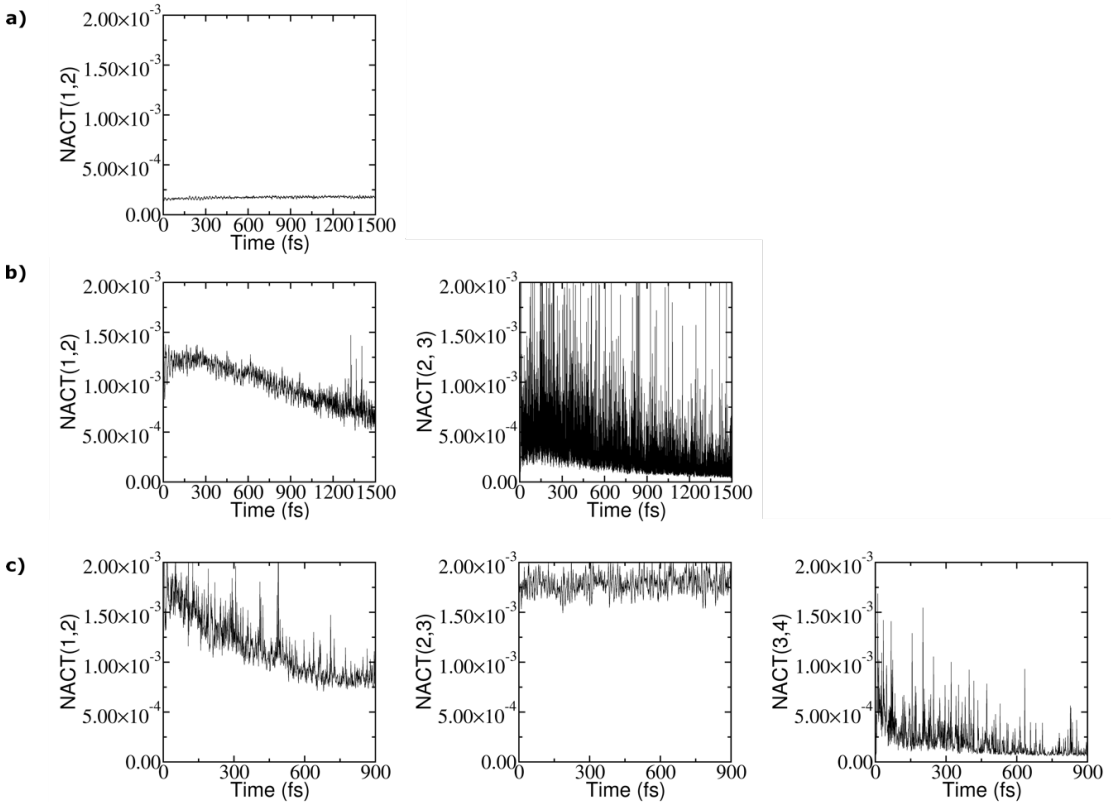

Figure S5. Average absolute values of the non-adiabatic coupling terms (NACT) during excited state non-adiabatic dynamics calculations of: a) monomer, b) dimer, and c) trimer.

6. Dimer active normal modes

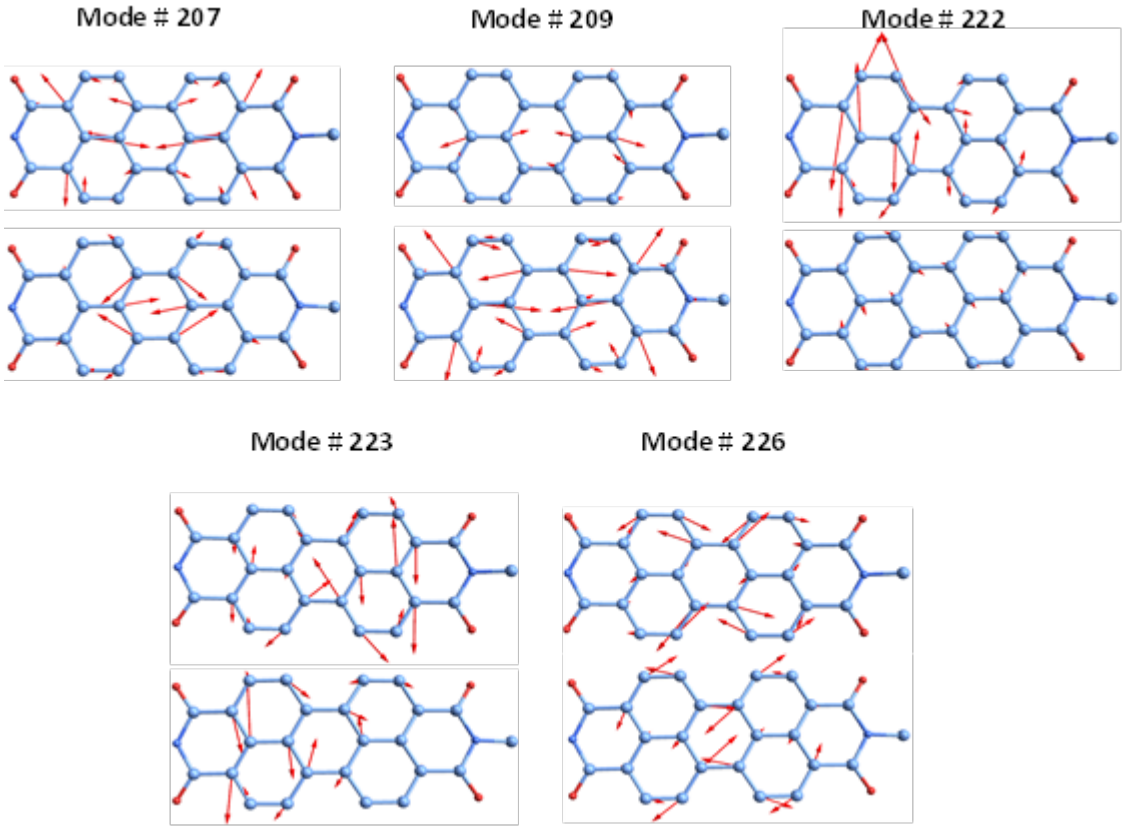

Figure S6. Representation of the normal modes that contribute the most to the $S_3 \rightarrow S_2$ and $S_2 \rightarrow S_1$ non-adiabatic electronic energy transfers during NEXMD simulations of the PDI dimer. For each normal mode, the motions associated to each monomer are ordered in columns.

7. Trimer active normal modes

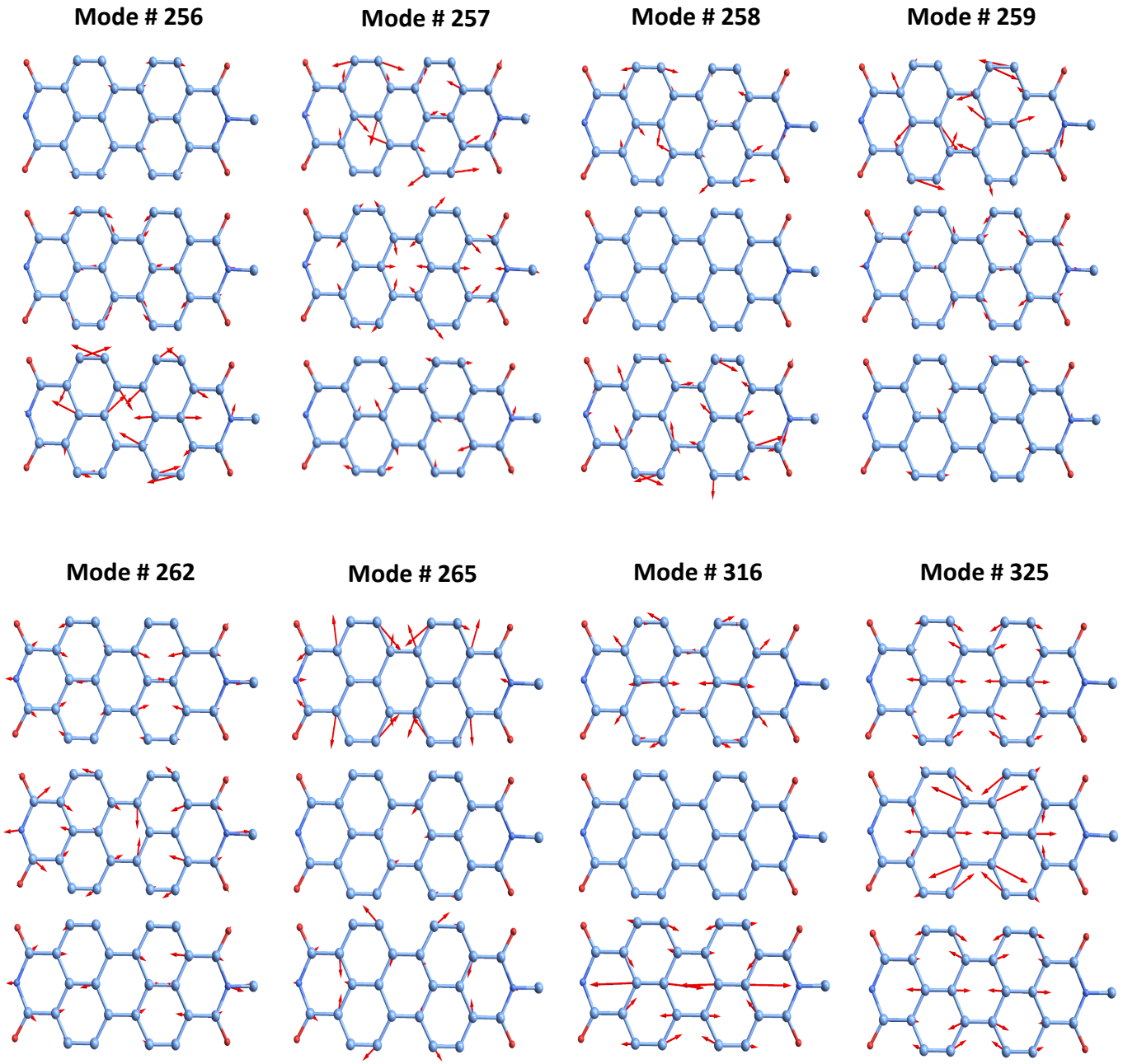

Figure S7. Representation of the normal modes that contribute the most to the $S_4 \rightarrow S_3$, $S_3 \rightarrow S_2$ and $S_2 \rightarrow S_1$ non-adiabatic electronic energy transfers during NEXMD simulations of the PDI trimer. For each normal mode, the motions associated to each monomer are ordered in columns.

8. Transition density for the dimer

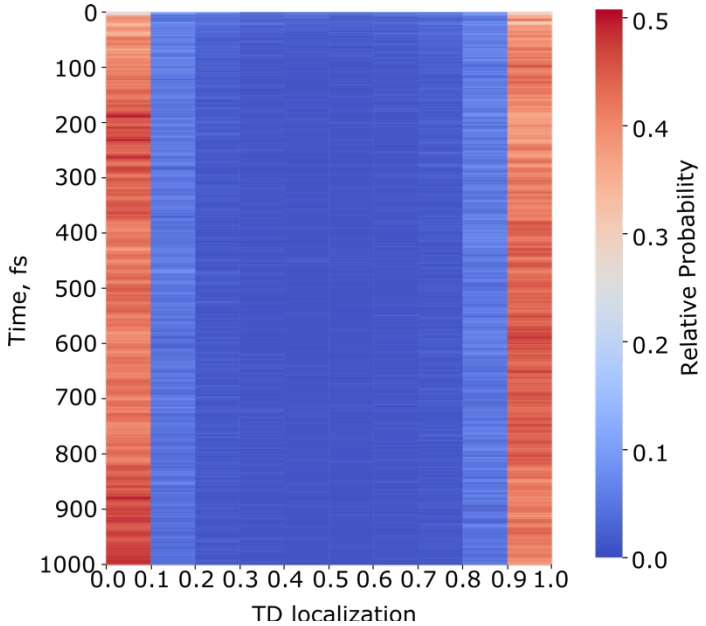

Figure S8. The localization of the transition density (TD) ($(p^{g\alpha})_X^2$) for the PDI dimer. The fraction of TD projected on one monomer is shown with relative probability defined as the number of trajectories with this projection.

9. Transition density for the trimer

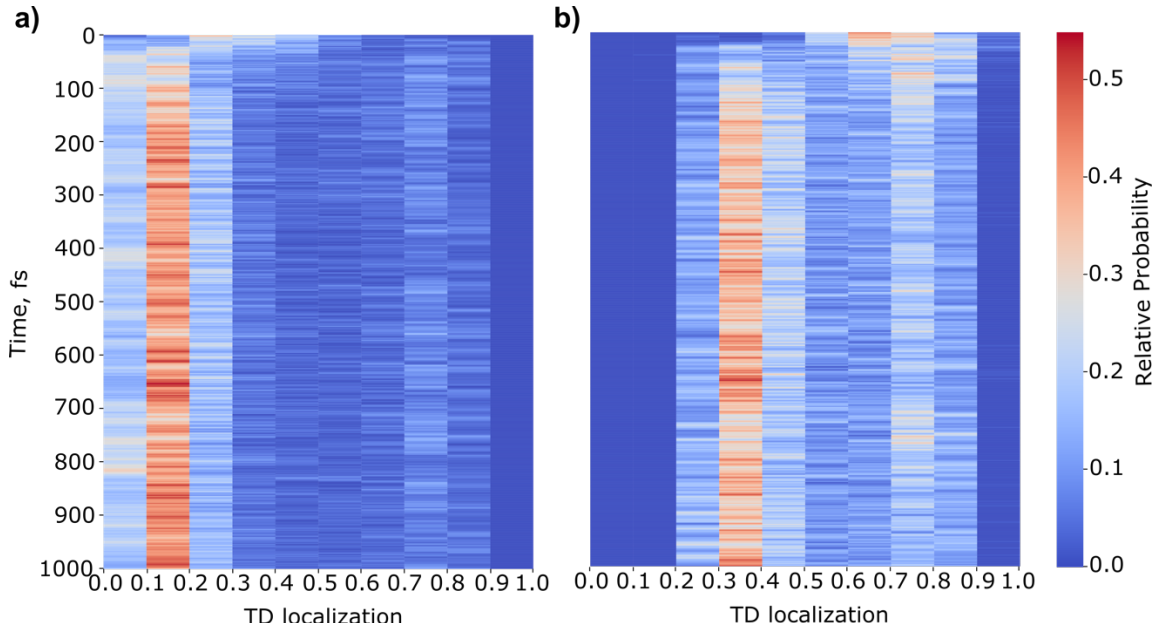

Figure S9. The localization of the transition density (TD) for the PDI trimer. For the trimer, the molecule is split in two parts: one dimer and one monomer as delineated in Figure S9. Figure S9(a) partitions the trimer into 1) top monomer and 2) dimer of the middle and bottom molecules. $(p^{g\alpha})_X^2 \sim 1$ indicates localization of the TD on the top monomer while $(p^{g\alpha})_X^2 \sim 0$ indicates localization on the bottom two molecules. Figure S9(b) partitions the trimer as consisting of the central monomer and the two outer monomers. In this case $(p^{g\alpha})_X^2 \sim 0$ indicates localization on either the top or bottom monomer or delocalization over both molecules while a value of $(p^{g\alpha})_X^2 \sim 1$ indicates localization on the middle monomer

10. Impact of backbone on absorption spectrum of dimer

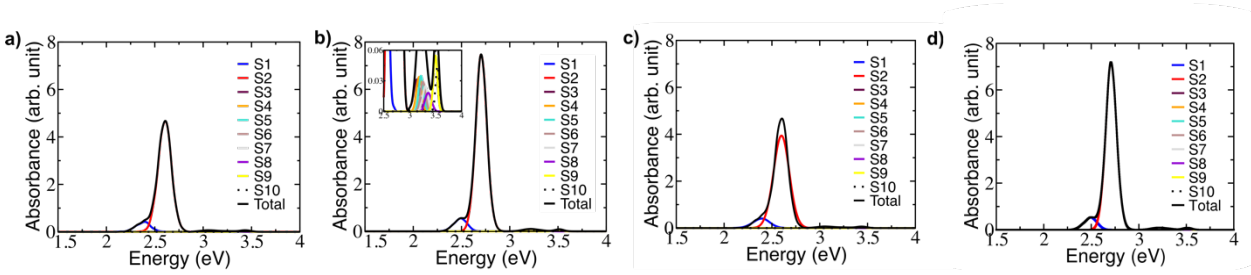

Figure S10. Absorption spectrum of a) optimized geometry of dimer b) dimer with backbone c) dimer with removed backbone, geometry was not optimized further and ground state MD sampling started from this initial geometry shown in the figure d) dimer without backbone. Here, backbone was removed and replaced with hydrogen for each trajectory with backbone obtained during ground state MD from case (b).

11. Non-adiabatic coupling terms for monomer with and without backbone

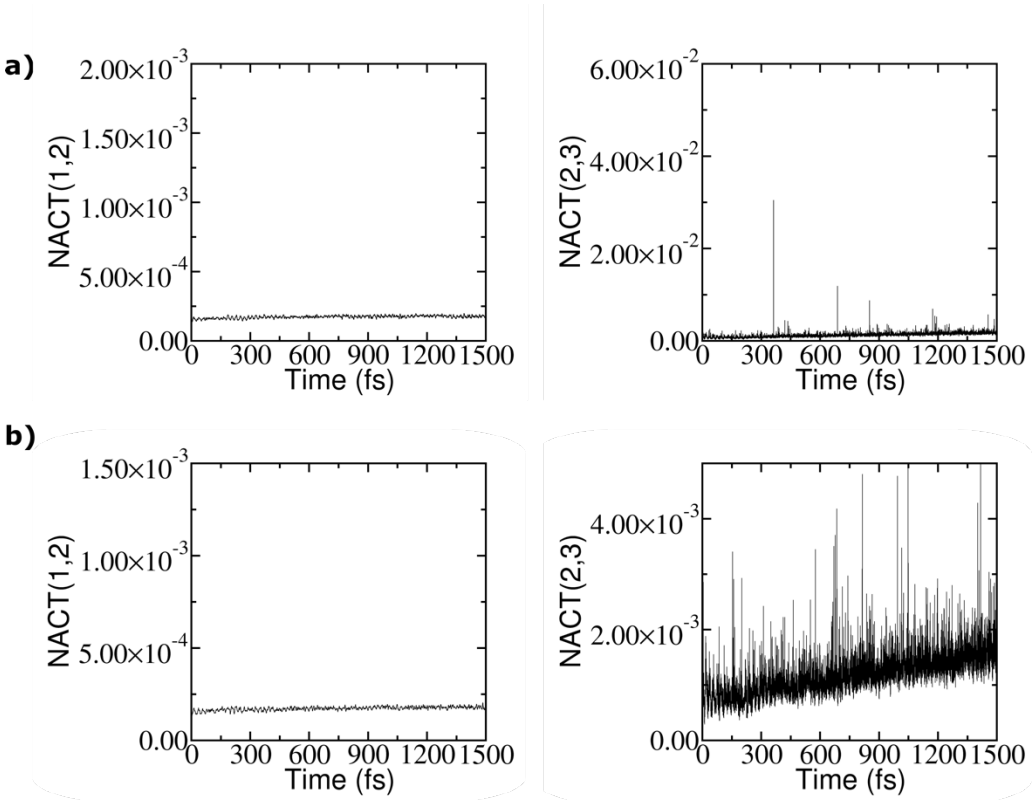

Figure S11. Average absolute values of the non-adiabatic coupling terms (NACT) during excited state non-adiabatic dynamics calculations of the a) monomer b) monomer with backbone

12. Non-adiabatic coupling terms for dimer with and without backbone

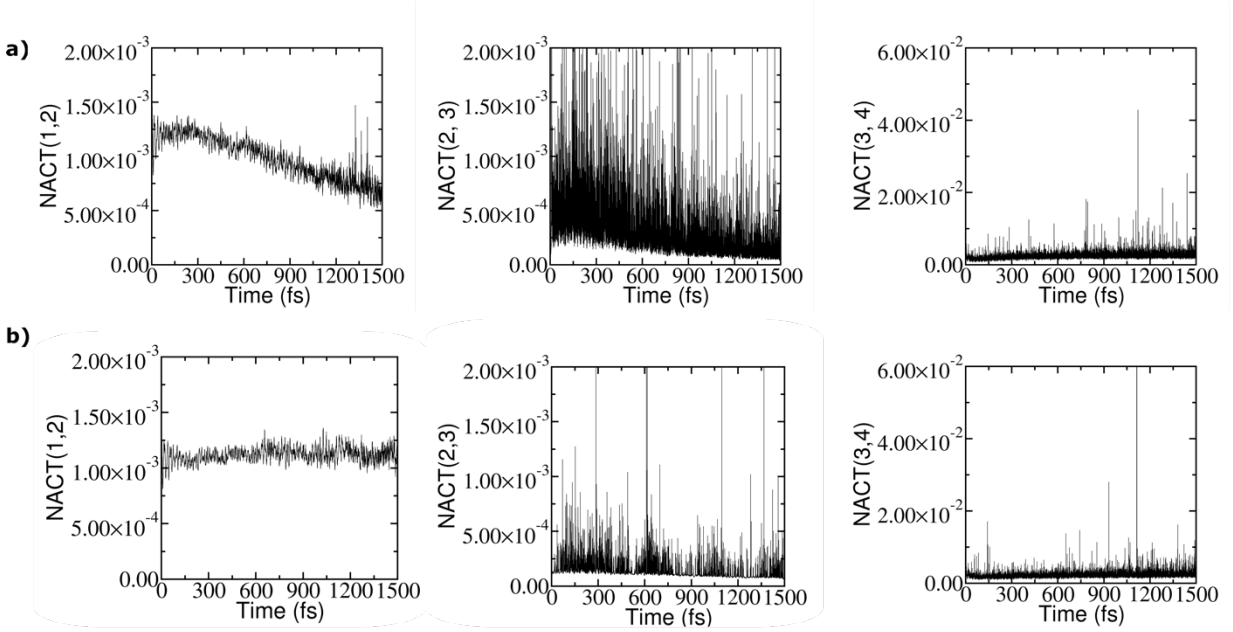

Figure S12. Average absolute values of the non-adiabatic coupling terms (NACT) during excited state non-adiabatic dynamics calculations of the a) dimer b) dimer with backbone

13. Comparison of population dynamics for three dimer cases

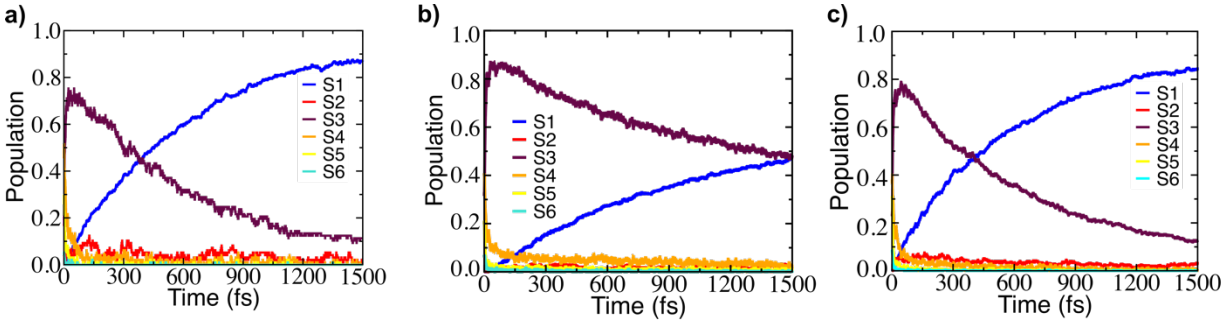

Figure S13. Population dynamics of a) optimized geometry of dimer b) dimer with backbone c) dimer with removed backbone, geometry was not optimized further and ground state MD sampling started from this initial geometry shown in the figure.

14. Transition density for the dimer with backbone

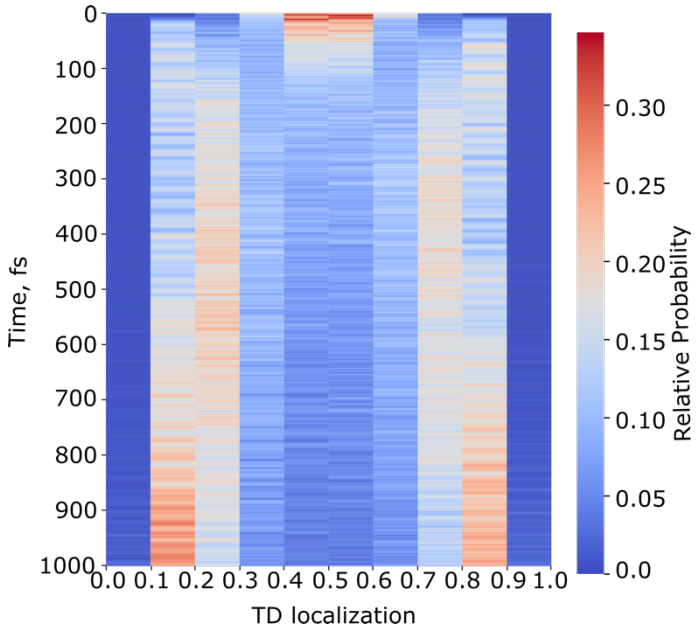

Figure S14. The localization of the transition density (TD) for the PDI dimer with backbone. For the dimer, the fraction of TD projected on one monomer is shown with relative probability defines as the number of trajectories with this projection.